symmetry

MDPI

Article

Hidden Euclidean Dynamical Symmetry in the U($n+1$) Vibron Model

Yu Zhang *, Zi-Tong Wang, Hong-Di Jiang and Xin Chen

Department of Physics, Liaoning Normal University, Dalian 116029, China
* Correspondence: dlzhangyu@lnnu.edu.cn

Abstract: Based on the boson realization of the Euclidean algebras, it is found that the E(n) dynamical symmetry (DS) may emerge at the critical point of the U(n)-SO($n+1$) quantum phase transition. To justify this finding, we provide a detailed analysis of the transitional Hamiltonian in the U($n+1$) vibron model in both quantal and classical ways. It is further shown that the low-lying structure of ^{82}Kr can serve as an excellent empirical realization of the E(5) DS, which provides a specific example of the Euclidean DS in experiments.

Keywords: Euclidean dynamical symmetry; vibron mode; critical point symmetry; quantum phase transition

Citation: Zhang, Y.; Wang, Z.-T.; Jiang, H.-D.; Chen, X. Hidden Euclidean Dynamical Symmetry in the U($n+1$) Vibron Model. *Symmetry* **2022**, *14*, 2219. https://doi.org/10.3390/sym14102219

Academic Editor: Alberto Ruiz Jimeno

Received: 28 September 2022
Accepted: 17 October 2022
Published: 21 October 2022

1. Introduction

Dynamical symmetries (DSs) play an essential role in deeply understanding dynamical structures of quantum many-body systems. In general, a DS is supposed to occur when the Hamiltonian of a system can be expressed as a combination of the Casimir operators of a chain of Lie group, $G \supset G' \supset G'' \cdots$ [1]. The DS of this type can be recognized by analyzing the associated algebraic structure. The typical examples are those associated with the interacting boson model (IBM) [2] and the U(4) vibron model [3]. In the IBM, there are three typical DSs, U(5), SO(6) and SU(3), with their group generators being all reduced from the U(6) ones, which are composed of 36 bilinear products of the s d boson operators [2]. Apart from the exact DSs, approximate DSs are suggested to exist in many-body systems too and yield some important symmetry-based concepts. For instance, the partial dynamical symmetries [4–6] and quasidynamical symmetries [7–9] have been found to occur in the IBM and other algebraic models. Approximate DSs are usually hidden behind a complicate parameter relation of the Hamiltonian of a given system. One example is just the SU(3) approximate symmetry in the IBM [10,11], which was found to be preserved along the trajectory in the IBM parameter space close to the Alhassid–Whelan arc of regularity [12].

There is another type of DS, called critical point symmetry (CPS) [13]. As the first example, the E(5) CPS was proposed to describe the spectra of nuclei around the critical point of the U(5)-SO(6) quantum phase transition (QPT) [13]. This mode was initially built in the Bohr–Mottelson model [14] with the collective potential function in the CPS Hamiltonian being taken as an infinite square well in order to simulate the case at the critical point of the U(5)-SO(6) QPT in the IBM [2]. In [15,16], the d-boson realization of the five-dimensional Euclidean DS was proposed, by which a much closer relation between the E(5) CPS and the U(5)-SO(6) QPT was revealed. The E(5) CPS has been further extended to the cases of $n = 3$ [17] and $n = 2$ [18,19] to describe other quantum phase transitional systems. In view of the success of the Euclidean mode as a benchmark for critical structure, it is necessary to provide a general analysis of how an Euclidean DS shows up in quantum many-body systems.

In this work, we will focus on a boson realization of the n-dimensional Euclidean algebra with $n = 2l + 1$ and $l = 0, 1, 2, \cdots$ and try to reveal the connection between the E(n) DS and the U($n+1$) vibron model [1] which is used to describe the 2^l-pole deformation

of a many-body system. The famous examples of the U($n+1$) vibron model are just the IBM (U(6)) describing the quadrupole deformation of nuclei [2] and the U(4) vibron model describing the spectra of diatomic molecules corresponding to a dipole-deformed system [3]. They are also two important examples that will be discussed in this work.

2. The Boson Realization of the E(n) Algebra

The n-dimensional Euclidean (E(n)) space with $n = 2l+1$ is generated by the coordinates $q_u^{(l)}$ ($u = 0,\ \pm1,\ \pm2,\ \pm l$), to which the conjugate momenta are defined as $p_u^{(l)} = -i\frac{\partial}{\partial q_u^{(l)}}$. The associated E($n$) group symmetry is then described as the invariance under the translations and rotations in the E(n) space [1]. For convenience, the symbols $p_u(q_u)$ will be used instead of $p_u^{(l)}(q_u^{(l)})$ in the following discussion. The other conventions are

$$\tilde{A}_u^{(\lambda)} = (-1)^{\lambda-u} A_{-u}^{(\lambda)}, \tag{1}$$

$$(A^{(\lambda)})^2 = \sum_u A_u^{(\lambda)} \tilde{A}_u^{(\lambda)} = (\tilde{A}^{(\lambda)})^2, \tag{2}$$

$$\tilde{A}^{(\lambda)} \cdot \tilde{A}^{(\lambda)} = \sum_u (-1)^u \tilde{A}_u^{(\lambda)} \tilde{A}_{-u}^{(\lambda)}, \tag{3}$$

$$(\tilde{A}^{(\lambda)} \times \tilde{B}^{(\lambda')})_{u''}^{(\lambda'')} = \sum_{uu'} \langle \lambda u \lambda' u' \mid \lambda'' u'' \rangle \tilde{A}_u^{(\lambda)} \tilde{B}_{u'}^{(\lambda')}, \tag{4}$$

in which $\tilde{A}_u^{(\lambda)}(\tilde{B}^{(\lambda)})$ represents a spherical tensor of spin λ. As we know, the E(n) group can be expressed as the semidirect product of R(n) and SO(n), namely

$$\mathrm{E}(n) = \mathrm{R}(n) \otimes_{\mathrm{s}} \mathrm{SO}(n), \tag{5}$$

where R(n) represents the n-dimensional translation group generated by $i\tilde{p}_u$ and SO(n) denotes the n-dimensional rotation group generated by $\hat{T}_u^{(k)} \equiv i(q \times \tilde{p})_u^{(k)}$ with $k = 1, 3, \cdots, 2l-1$. The kinetic energy term $p^2 = \sum_u \tilde{p}_u p_u$ is shown to be an invariant quantity of the E(n) group with $[i\tilde{p}_u,\ p^2] = 0$ and $[\hat{T}_u^{(k)},\ p^2] = 0$. Considering the conservation of angular momentum, the E(n) DS in a many-body system may be characterized by the group chain

$$\mathrm{E}(n) \supset \mathrm{SO}(n) \supset \mathrm{SO}(3) \tag{6}$$

with the angular momentum group SO(3) being generated by $\hat{T}_u^{(1)}$.

To build a boson realization of the E(n) algebra, one can define the boson operators of spin l by

$$b_u^{l\dagger} = \frac{1}{\sqrt{2}}[q_u - i\tilde{p}_u],\ \ b_u^l = \frac{1}{\sqrt{2}}[\tilde{q}_u + ip_u], \tag{7}$$

where $l = 0,\ 1,\ 2, \cdots$ stands for the boson type, $s,\ p,\ d, \cdots$. The definition in (7) is a direct extension of the $l = 2$ case in [20]. With this definition, it is easy to prove the boson commutation relation, $[b_{u'}^{l'},\ b_u^{l\dagger}] = \delta_{u'u}\delta_{l'l}$. The $n(n+1)/2$ generators of the E(n) Lie algebra are then rewritten as

$$\hat{\Lambda}_u^{(l)} \equiv i\tilde{p}_u = \frac{1}{\sqrt{2}}[\tilde{b}_u^l - b_u^{l\dagger}], \tag{8}$$

$$\hat{T}_u^{(k)} \equiv i(q \times \tilde{p})_u^{(k)} = (b^{l\dagger} \times \tilde{b}^l)_u^{(k)},\ \ k = 1,\ 3,\ \cdots,\ 2l-1. \tag{9}$$

The 2nd-order Casimir operator of the E(n) group is given by

$$\hat{C}_2[\mathrm{E}(n)] \equiv p^2 = \hat{n}_{b^l} + \frac{n}{2} - \frac{1}{2}(-)^l\left(\hat{P}_l^\dagger + \hat{P}_l\right) \tag{10}$$

with

$$\hat{n}_{b^l} = \sum_u b_u^{l\dagger} b_u^l, \quad \hat{P}_l = \sum_u (-)^u \tilde{b}_u^l \tilde{b}_{-u}^l, \quad \hat{P}_l^\dagger = (\hat{P}_l)^\dagger . \tag{11}$$

It can be proved that these generators satisfy the commutation relations:

$$[\hat{\Lambda}_u^{(l)}, \hat{\Lambda}_v^l] = 0 , \tag{12}$$

$$[\hat{T}_u^{(k)}, \hat{\Lambda}_v^{(l)}] = -\sqrt{\frac{(2k+1)}{2l+1}} \langle kulv|lu+v\rangle \hat{\Lambda}_{u+v}^{(l)} , \tag{13}$$

$$[\hat{T}_u^{(k)}, \hat{T}_{\bar{u}}^{(\bar{k})}] = -2\sqrt{(2k+1)(2\bar{k}+1)} \sum_{\lambda=\text{odd}} \left\{ \begin{array}{c} k, \bar{k}, \lambda \\ l,\ l,\ l \end{array} \right\} \times \langle ku\bar{k}\bar{u}|\lambda u+\bar{u}\rangle \ \hat{T}_{u+\bar{u}}^{(\lambda)} , \tag{14}$$

and

$$\left[\hat{\Lambda}_u^{(l)},\ \hat{C}_2[\mathrm{E}(n)]\right] = \left[\hat{T}_u^{(k)},\ \hat{C}_2[\mathrm{E}(n)]\right] = 0 . \tag{15}$$

Clearly, n is an odd number with $n = 2l+1$ and $\mathrm{E}(n)$ is a non-compact Lie group.

3. The U($n+1$) Algebra and Group Contraction

The U$(n+1)$ vibron model with $n = 2l+1$ can be applied to describe the 2^l-pole deformation dynamics of a many-body system [1]. The Hamiltonian in the U$(n+1)$ vibron model is constructed from two kinds of boson operators: the scalar s-boson and the l-th rank tensor b^l-boson. Then, the $(n+1)^2$ bilinear operators

$$s^\dagger s, \quad s^\dagger b_u^l, \quad b_u^{l\dagger} s, \quad b_u^{l\dagger} b_v^l \quad u,\ v = -l,\ -l+1,\ \cdots,\ l \tag{16}$$

may generate the maximal dynamical symmetry group, U$(n+1)$. One of its subgroups is just U(n) generated by

$$\hat{B}_q^{(k)} = (b^{l\dagger} \times \tilde{b}^l)_q^{(k)}, \quad k = 0,\ 1,\ 2,\ \cdots,\ 2l \tag{17}$$

with the algebraic relation

$$[\hat{B}_u^{(k)}, \hat{B}_{\bar{u}}^{(\bar{k})}] = \sqrt{(2k+1)(2\bar{k}+1)} \sum_\lambda \left\{ \begin{array}{c} k, \bar{k}, \lambda \\ l,\ l,\ l \end{array} \right\} \times \left((-)^\lambda - (-)^{k+\bar{k}}\right) \langle ku\bar{k}\bar{u}|\lambda u+\bar{u}\rangle \hat{B}_{u+\bar{u}}^{(\lambda)} \tag{18}$$

and another one is SO$(n+1)$ generated by

$$\hat{Q}_u = (s^\dagger \times \tilde{b}^l + b^{l\dagger} \times \tilde{s})_u^{(l)}, \quad \hat{T}_q^{(k)} = \hat{B}_q^{(k)}, \quad k = \text{odd} \tag{19}$$

with the algebraic relation

$$[\hat{Q}_u,\ \hat{Q}_v] = 2\sum_k \langle lulv|ku+v\rangle \hat{T}_{u+v}^{(k)} , \tag{20}$$

$$[\hat{T}_u^{(k)}, \hat{Q}_v] = -\sqrt{\frac{2k+1}{2l+1}} \langle kulv|lu+v\rangle \hat{Q}_{u+v} . \tag{21}$$

Note that $[\hat{T}_u^{(k)}, \hat{T}_{\bar{u}}^{(\bar{k})}]$ is already given in (14). Clearly, SO(n) is the common subgroup of U(n) and SO($n+1$). Accordingly, two typical DSs in the U($n+1$) vibron model can be characterized by the group chains [1]

$$\mathrm{U}(n+1) \supset \mathrm{U}(n) \supset \mathrm{SO}(n) \supset \mathrm{SO}(3)\,, \tag{22}$$
$$\mathrm{U}(n+1) \supset \mathrm{SO}(n+1) \supset \mathrm{SO}(n) \supset \mathrm{SO}(3)\,. \tag{23}$$

The relevant Casimir operators are defined by

$$\hat{C}_1[\mathrm{U}(n)] = \hat{n}_{b^l}, \tag{24}$$
$$\hat{C}_2[\mathrm{U}(n)] = \hat{n}_{b^l}(\hat{n}_{b^l} + n - 1), \tag{25}$$
$$\hat{C}_2[\mathrm{SO}(n+1)] = (-1)^l \hat{Q} \cdot \hat{Q} + 2\sum_k \hat{T}^{(k)} \cdot \hat{T}^{(k)}, \tag{26}$$
$$\hat{C}_2[\mathrm{SO}(n)] = 2\sum_k \hat{T}^{(k)} \cdot \hat{T}^{(k)}, \tag{27}$$
$$\hat{C}_2[\mathrm{SO}(3)] = \frac{l(l+1)(2l+1)}{3}\hat{T}^{(1)} \cdot \hat{T}^{(1)}\,, \tag{28}$$

where the operators $\hat{n}_{b^l}$, $\hat{Q}_u$ and $\hat{T}_u^{(k)}$ are defined in (11) and (19). The corresponding eigenvalues can be expressed as

$$\langle \hat{C}_1[\mathrm{U}(n)] \rangle = n_{b^l}, \tag{29}$$
$$\langle \hat{C}_2[\mathrm{U}(n)] \rangle = n_{b^l}(n_{b^l} + n - 1), \tag{30}$$
$$\langle \hat{C}_2[\mathrm{SO}(n+1)] \rangle = \sigma(\sigma + n - 1), \tag{31}$$
$$\langle \hat{C}_2[\mathrm{SO}(n)] \rangle = \omega(\omega + n - 2), \tag{32}$$
$$\langle \hat{C}_2[\mathrm{SO}(3)] \rangle = L(L+1) \tag{33}$$

with the quantum numbers n_{b^l}, σ, ω, and L being used to signify the irreducible representations of U(n), SO($n+1$), SO(n) and SO(3), respectively [1].

It is interesting to find that the SO($n+1$) algebraic structure is very similar to the E(n) one. Both of them have the SO(n) algebra as their subalgebra. If the generators are rescaled by [11]

$$\hat{q}_u = \frac{1}{\sqrt{C_2[\sigma]}}\hat{Q}_u \tag{34}$$

with $C_2[\sigma] = \sigma(\sigma + 2l)$, the algebraic relation shown in (21) and (20) will be changed into

$$[\hat{T}_u^{(k)}, \hat{q}_v] = -\sqrt{\frac{2k+1}{2l+1}}\langle kulv|lu+v\rangle \hat{q}_{u+v}, \tag{35}$$
$$[\hat{q}_u, \hat{q}_v] = 2\sum_k \langle lulv|ku+v\rangle \frac{1}{C_2[\sigma]}\hat{T}_{u+v}^{(k)}\,. \tag{36}$$

In the $\sigma \to \infty$ limit, it is given by $[\hat{q}_u, \hat{q}_v] \simeq 0$ for small ω cases, in which the expectation values $\langle \hat{T}(k) \rangle$ should be small. By this procedure, one may obtain the same commutation relations as those shown in (12)–(14) with the correspondence $\hat{\Lambda} \to \hat{q}$. It means that the SO($n+1$) $\to$ E(n) contraction may happen in the $\sigma \to \infty$ limit. Such a group contraction for $n = 5$ was previously discussed in [11] and earlier in [21]. The present result is a direct generalization of the $n = 5$ case. Another example worth mentioning is SU(3) $\to$ R(5) $\otimes_s$ SO(3), which can be achieved via a similar procedure [11,22]. This group contraction provides the theoretical basis to construct the SU(3) image of the triaxial rotor dynamics [23,24], which offers a microscopic way of understanding collective rotations in triaxial nuclei based on the SU(3) shell model [25,26]. Different aspects of the SU(3) symmetry in nuclei are introduced in [22].

4. The Emergent E(n) DS in the U(n)-SO($n+1$) QPT

In contrast to the group contraction, we hope to emphasize in this work another way in which the E(n) symmetry can dynamically emerge from the U($n+1$) vibron model. As discussed above, U(n) and SO($n+1$) are two typical dynamical symmetry limits in the vibron model. The Hamiltonian for either of them can be written as a linear combination of the Casimir operators of the corresponding group chain so that the eigenvalues and eigenvectors can be expressed in an analytical way (see Equations (29)–(33)). In general, no analytical solutions can be achieved in the cases of symmetry mixing. Nevertheless, beautiful algebraic solutions of the Hamiltonian mixing the U(n) and O($n+1$) DSs have been obtained in [27,28] using the Bethe ansatz within an infinite-dimensional Lie algebra.

4.1. The Transitional Hamiltonian

To discuss a general situation in the U($n+1$) vibron model, we adopt here a schematic Hamiltonian

$$\begin{aligned} \hat{H} &= \varepsilon\Big[(1-\eta)\hat{n}_{b^l} - \frac{\eta}{4N}(-1)^l \hat{Q}\cdot\hat{Q}\Big] \\ &= \varepsilon\Big[(1-\eta)\hat{C}_1[\mathrm{U}(n)] - \frac{\eta}{4N}\hat{C}_2[\mathrm{SO}(n+1)] \\ &\quad + \frac{\eta}{4N}\hat{C}_2[\mathrm{SO}(n)]\Big], \end{aligned} \tag{37}$$

where $N = n_s + n_{b^l}$ represents the total boson number of the system and ε is a scale parameter to be set with $\varepsilon = 1$ in the discussions. It is apparent that the system is in the U(n) DS when the control parameter $\eta = 0$ and is changed into the SO($n+1$) DS when $\eta = 1$. By varying $\eta \in [0, 1]$, the Hamiltonian (37) describes a transitional situation in between the U(n) and SO($n+1$) symmetry limits. In addition to U(n) and SO($n+1$), there may exist other DSs in the U($n+1$) vibron model for $n \geq 5$. For example, the SU(3) DS will be involved in the $n = 5$ case [2]. Nonetheless, it is sufficient to discuss the cases involving the U(n) and SO($n+1$) DSs for the present purpose. The reason is that the SO(n) $\supset$ SO(3) DS (see Equation (6)) will be conserved in the vibron model only in the U(n) and SO($n+1$) limits or their mixing. Therefore, one only needs to analyze the transitional Hamiltonian, such as that given in (37) to reveal the underlying E(n) DS in the U($n+1$) vibron model.

4.2. Quantal Analysis

As is known [11], if a system has an underlying symmetry of the group G, the corresponding Hamiltonian should commute with all the generators of group G. To identify the underlying E(n) DS in the parameter space of the vibron model, we examine the commutation relations between the generators of the E(n) group defined in (8) and (9) and the Hamiltonian (37). First of all, one can derive that

$$[\hat{T}^{(k)}_u,\ \hat{n}_{b^l}] = 0, \tag{38}$$

$$[\hat{\Lambda}^{(l)}_u,\ \hat{n}_{b^l}] = \frac{1}{\sqrt{2}}(\tilde{b}^l_u + b^{l\dagger}_u), \tag{39}$$

$$[\hat{\Lambda}^{(l)}_u,\ \hat{Q}_v] = \frac{(-)^{l-u}}{\sqrt{2}}\delta_{u,-v}(s + s^\dagger)\,. \tag{40}$$

With the commutators, it is easy to prove $[\hat{T}^{(k)}_u,\ \hat{H}]=0$. This point actually reflects the fact that $\hat{T}^{(k)}_u$ as the generators of U(n) and SO($n+1$) should commute with their Casimir operators. Furthermore, one can derive in the $\langle \hat{n}_{b^l}/N\rangle \to 0$ limit that

$$\begin{aligned}[\hat{\Lambda}^{(l)}_u,\ \hat{H}] &= \frac{\sqrt{2}}{2}(1-\eta)(\tilde{b}^l_u + b^{l\dagger}_u)\\ &- \frac{\sqrt{2}\eta}{4N}\left(s^\dagger s^\dagger \tilde{b}^l_u + ss b^{l\dagger}_u + s^\dagger s \tilde{b}^l_u + ss^\dagger b^{l\dagger}_u\right)\\ &\approx |_{\langle \hat{n}_{b^l}/N\rangle\to 0}\ \frac{\sqrt{2}}{2}(1-2\eta)(\tilde{b}^l_u + b^{l\dagger}_u)\,. \end{aligned} \tag{41}$$

In the derivation, we used the replacements

$$\begin{aligned} s^\dagger(s) &\to \sqrt{n_s+1}(\sqrt{n_s})\\ &= \sqrt{N-n_{b^l}+1}(\sqrt{N-n_{b^l}}) \simeq \sqrt{N}\,, \end{aligned} \tag{42}$$

which should be well satisfied in the $\langle \hat{n}_{b^l}/N\rangle \to 0$ limit due to $N = n_{b^l} + n_s$. It is clear that the commutator given in (41) will vanish at $\eta = 1/2$. Therefore, we conclude that the vibron Hamiltonian (37) at the parameter point $\eta = 1/2$ is invariant under the E(n) group transformations when $\langle \hat{n}_{b^l}/N\rangle \to 0$. In other words, the E($n$) DS will occur in the U(n)-SO($n+1$) transitional region under this approximate condition.

To examine the required condition for the E(n) DS, we take $n = 3$ and $n = 5$ to represent the examples of $l =$ odd and $l =$ even, respectively. For $n = 5$, the U($n+1$) vibron model is reduced to the IBM (U(6)) [2]. Accordingly, the Hamiltonian in (37) can be used to describe nuclear structural evolution from the spherical vibration (U(5) DS) to γ-unstable rotation (SO(6) DS). To solve this Hamiltonian, one can diagonalize it within the U(5) basis of the IBM

$$|\ \phi\rangle_{\mathrm{U}(5)} = |\ N\ n_d\ \tau\ \Delta\ L\rangle\,. \tag{43}$$

Here, N, n_d, τ and L represent the quantum numbers for U(6), U(5), SO(5) and SO(3), while Δ denotes the additional quantum number in the reduction SO(5)$\supset$SO(3) [2]. With the solved wavefunctions, one can calculate the expectation value $\rho(\eta) = \langle \phi\ |\ \hat{n}_d/N\ |\ \phi\rangle$ for any given state $|\ \phi\rangle$ to check the condition $\langle \hat{n}_{b^l}/N\rangle \to 0$. If taking $n = 3$, the U(4) vibron model for molecular spectra is obtained with the Hamiltonian in (37) being used to describe the U(3)-SO(4) transition [3]. Similarly, one can worked out the expectation value $\rho(\eta)$ through diagonalizing the transitional Hamiltonian within the U(3) basis

$$|\ \phi\rangle_{\mathrm{U}(3)} = |\ N\ n_p\ L\rangle\,, \tag{44}$$

where N, n_p and L represent the quantum numbers for U(4), U(3) and SO(3), respectively [3]. In (43) and (44), the quantum number of the angular momentum projection, M, is ignored for convenience.

In Figure 1, the evolutions of $\rho(\eta)$ for the lowest states with $L = 0, 2, 4$ are shown for both the U(4) and U(6) models. The total boson numbers in the two models are both taken as $N = 100$. One can find from Figure 1 that $\rho(\eta)$ in the two models exhibit nearly the same evolutional behaviors. Specifically, the values of ρ as a function of η remain with $\rho \sim 0$ for $\eta \in [0,\ 1/2]$ and rapidly increase when $\eta > 1/2$. It is thus justified that the condition $\langle \hat{n}_{b^l}/N\rangle \to 0$ is well satisfied in the present cases. In particular, the larger the boson number N, the better the approximation $\langle \hat{n}_{b^l}/N\rangle \to 0$. If $N \to \infty$, the condition $\langle \hat{n}_{b^l}/N\rangle = 0$ at $\eta = 1/2$ will be exactly achieved for the ground state as discussed later, which means that E(n) could be an exact ground-state DS in the vibron model in the large N limit. In addition, the sudden enhancements in $\rho(\eta)$ as shown in Figure 1 actually manifests that this is a precursor of the U(n)-SO($n+1$) QPT defined in the large-N limit.

According to the Ehrenfest classification, such an QPT is suggested to be of the second order. That is, the ground state energy E_g and its first derivative, $\frac{\partial E_g}{\partial \eta}$, are both continuous at the transitional point but the second derivative, $\frac{\partial^2 E_g}{\partial \eta^2}$, is discontinuous [2]. Based on the Hellmann–Feynman theorem, $\frac{\partial E_n}{\partial \eta} = \langle \frac{\partial H}{\partial \eta} \rangle_n$, one can further derive that

$$\frac{\partial e_g}{\partial \eta} = \frac{1}{\eta}(e_g - \rho(\eta)_g), \quad \frac{\partial^2 e_g}{\partial \eta^2} = -\frac{1}{\eta}\frac{\partial \rho(\eta)_g}{\partial \eta}, \tag{45}$$

where $e_g \equiv E_g/N$ represents the ground state energy per boson. It is thus suggested that the quantity $\rho(\eta)_g = \langle \hat{n}_b^l/N \rangle_g$ may serve as a quantum order parameter [29] for the U(n)-SO($n+1$) QPT. As seen in Figure 1, one can locate the critical point of this QPT at $\eta_c = 1/2$. It means that the E(n) DS may also play a role of critical point symmetry (CPS) in the U($n+1$) vibron model [13,30].

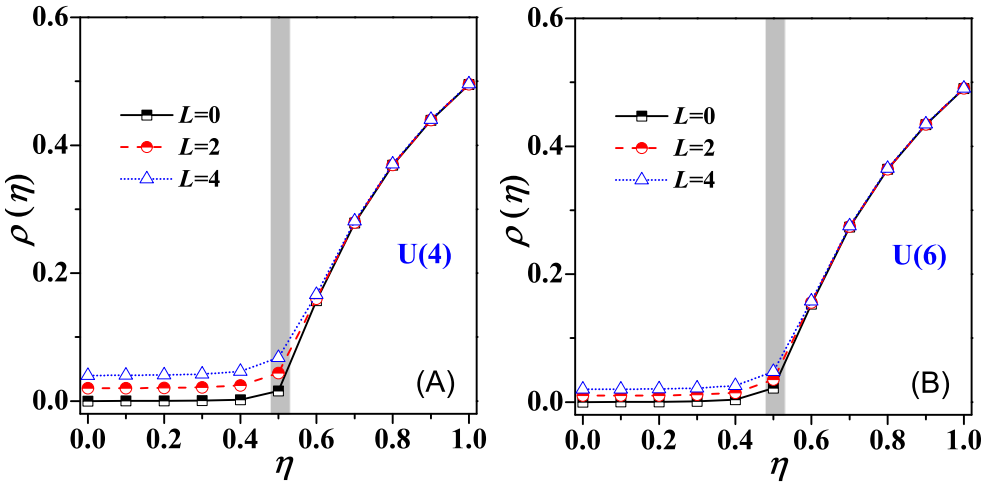

Figure 1. (**A**) The order parameter $\rho(\eta) = \langle \hat{n}_b^l \rangle / N$ changes as a function of η with the results solved from the U(4) model with $N = 100$ for the lowest states of $L = 0,\ 2,\ 4$. (**B**) The same as in (**A**) but for those solved from the U(6) model.

4.3. Classical Analysis

In the following, we will give a classical analysis of the transitional Hamiltonian (37) to further justify the hidden E((n)) DS. In the definitions (7), one can extract the scalar boson operator in terms of the one-dimensional coordinate and momentum [20]

$$s^\dagger = \frac{1}{\sqrt{2}}[q_s - ip_s], \quad s = \frac{1}{\sqrt{2}}[q_s + ip_s]\,. \tag{46}$$

The inverse transformations

$$q_s = \frac{1}{\sqrt{2}}[s^\dagger + s], \quad p_s = \frac{i}{\sqrt{2}}[s^\dagger - s] \tag{47}$$

indicate $q_s = \tilde{q}_s$ and $p_s = \tilde{p}_s$. Then, the transitional Hamiltonian (37) in the classical limit can be expressed as

$$\begin{aligned} H(q,p,q_s,p_s) &= (1-\eta)\frac{1}{2}\sum_u (q_u - i\tilde{p}_u)(\tilde{q}_u + ip_u) \\ &- \frac{\eta}{4N}(-1)^l Q(q,p,q_s,p_s)\cdot Q(q,p,q_s,p_s) \end{aligned} \tag{48}$$

with

$$Q = \frac{1}{2}\Big[(q_u - i\tilde{p}_u)(q_s + ip_s) + (q_s - ip_s)(q_u + i\tilde{p}_u))\Big]\,. \tag{49}$$

For the classical system, the operators $q_u,\ p_u,\ q_s,\ p_s$ become the ordinary coordinates and momenta. Then, the classical Hamiltonian is reduced to

$$\begin{aligned} H(q,p,q_s,p_s) &= \frac{1-\eta}{2}(q^2+p^2) \\ &- \frac{\eta}{4N}\Big[q^2q_s^2 + p^2p_s^2 + 2p_sq_s\sum_u(p_uq_u)\Big]\,. \end{aligned} \tag{50}$$

Accordingly, the boson number conservation condition $N = n_s + n_b$ leads to the classical constraint

$$\frac{1}{2}(q^2+p^2+q_s^2+p_s^2) = N\,. \tag{51}$$

With the condition $n_b/N \to 0$ indicating $s^\dagger(s) \simeq \sqrt{N}$, one may obtain $p_s = 0$ and $q_s = \sqrt{2N}$ (see Equation (47)). Then, the classical Hamiltonian (50) is further reduced to

$$H(q,p,q_s=\sqrt{2N},p_s=0) \simeq \frac{1-2\eta}{2}q^2 + \frac{1-\eta}{2}p^2\,. \tag{52}$$

It is easy to be deduced from (52) that the Hamiltonian describes an n-dimensional harmonic oscillator with

$$H\,|_{\eta=0} = \frac{1}{2}(q^2+p^2) \tag{53}$$

when $\eta = 0$ and describes an E(n) DS system with

$$H\,|_{\eta=\frac{1}{2}} = \frac{1}{4}p^2 = \frac{1}{4}\hat{C}[\mathrm{E}(n)] \tag{54}$$

when $\eta = 1/2$. Obviously, the E(n) DS in its classical limit just describes a free Hamiltonian [30]. It is thus justified that the E(n) DS may also hide in the classical system described by the same Hamiltonian under the same condition. Note that the approximation condition $n_b/N \to 0$ is not satisfied for $\eta > 1/2$, which means that one cannot derive the classical limit of the SO($n+1$) DS from (52) at $\eta = 1$.

In the quantal analysis, the condition $n_b/N \to 0$ is checked in a numerical way. In the following, we will identify this condition at the mean-field level. To do that, one needs to work out the scaled classical potential, which can be derived from the Hamiltonian (48) and given as

$$\begin{aligned} V(q,q_s) &\equiv \frac{1}{N}H(q,p,q_s,p_s)\,|_{p=0,p_s=0} \\ &= \frac{1-\eta}{2N}q^2 - \frac{\eta}{4N^2}q^2q_s^2\,. \end{aligned} \tag{55}$$

The truly classical limit is obtained for $N \to \infty$ with the inverse of the boson number $1/N$ playing a role of $\hbar$ [12,31]. So, we rescale here the coordinates with $\bar{q} = q/\sqrt{N}$ and $\bar{q_s} = q_s/\sqrt{N}$. The constraint condition in (51) is now changed into

$$\frac{1}{2}(\bar{q}^2 + \bar{q}_s^2) = 1\,, \tag{56}$$

by which the scaled potential is further reduced to

$$V(\bar{q}) = (\frac{1}{2} - \eta)\bar{q}^2 + \frac{\eta}{4}\bar{q}^4 \tag{57}$$

with $\bar{q}^2 \leq 2$. To see the deformation dependence of the potential, one should transform it into the intrinsic coordinate system through a rotation with Euler angles Ω,

$$\bar{q}_u = \sum_v D^{(l)}_{u,v}(\Omega)\bar{\beta}_v\,, \tag{58}$$

where $D^{(l)}$ are the Wigner matrices of spin l and $\bar{\beta}_v$ represent the intrinsic coordinates. However, this transformation may generate $\bar{q}^2 = \bar{\beta}^2$ and $\bar{q}^4 = \bar{\beta}^4$, which leaves the potential function form unchanged with

$$V(\bar{\beta}) = (\frac{1}{2} - \eta)\bar{\beta}^2 + \frac{\eta}{4}\bar{\beta}^4\,. \tag{59}$$

It means that the classical potential is only a function of the intrinsic "deformation" measured by $\bar{\beta} = \sqrt{\bar{\beta}^2}$. By further minimizing the potential with respect to $\bar{\beta}$, one can obtain the ground state energy per boson

$$e_g(\eta) \equiv V(\eta, \bar{\beta}_e) = \begin{cases} 0\,, & 0 \leq \eta \leq 1/2\,, \\ -\frac{(1-2\eta)^2}{4\eta}\,, & \eta > 1/2\,, \end{cases} \tag{60}$$

where $\bar{\beta}_e$ denotes the optimal value of $\bar{\beta}$, namely the ground state deformation. According to the Ehrenfest classification, one can prove that there exists a second-order QPT occurring at the parameter point $\eta = 1/2$, i.e., the U(n)-SO($n+1$) QPT. As noted above, the E(n) DS may occur at the same parameter point $\eta = 1/2$. It is thus confirmed that the Euclidean symmetry can indeed serve as a critical point symmetry.

For the U(n)-SO($n+1$) QPT, the ground state deformation $\bar{\beta}_e$ can be taken as the classic order parameter [29]. Its values can be derived as

$$\bar{\beta}_e(\eta) = \begin{cases} 0\,, & 0 \leq \eta \leq 1/2\,, \\ \sqrt{2(\eta - 1/2)/\eta}\,, & \eta > 1/2\,. \end{cases} \tag{61}$$

Then, one can extract the critical exponent $u = 1/2$ by expanding the order parameter around the critical point η_c [17] with

$$[\bar{\beta}_e(\eta) - \bar{\beta}_e(\eta_c)] \propto (\eta - \eta_c)^u\,. \tag{62}$$

Based on the relation given in (45), one can further work out $\rho(\eta)_g$ in the large-N limit (classical limit), which is given by

$$\rho(\eta)_g = \begin{cases} 0\,, & 0 \leq \eta \leq 1/2\,, \\ \frac{(2\eta-1)}{2\eta}\,, & \eta > 1/2\,. \end{cases} \tag{63}$$

The results indicate that the condition $\langle \hat{n}^l_b/N \rangle \to 0$ is strictly established in the large N limit for $\eta \in [0, 1/2]$. Moreover, the evolution feature of $\rho(\eta)_g$ shown in Figure 2 confirms that those presented in Figure 1 are indeed the finite-N precursors of the U(n)-SO($n+1$) QPT defined in the classical limit, which in turn justifies the consistency between the quantal analysis and classical analysis. It should be mentioned that one may obtain similar results by using other mean-field techniques, such as the coherent state method adopted in [32], where a classical analysis of the phase structure of the interacting boson models in arbitrary dimension was provided.

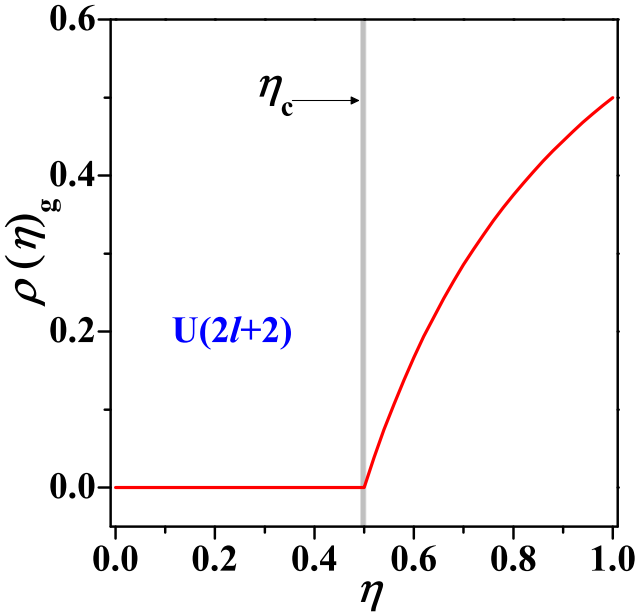

Figure 2. The evolution of $\rho(\eta)_g = \langle n_b^l/N\rangle_g$ as a function of η with the analytical expression given in (63).

5. An Example of the E(5) DS

As is known, the concept of CPS was proposed [13,33] in the framework of the Bohr–Mottelson model with the model predictions being well recognized in experiments [34–37]. Theoretically, the CPS method was extensively developed and became a "standard" way in modeling transitional structures of even–even nuclei [38–51], odd–A nuclei [52–58] and odd–odd nuclei [59]. The relevant case in this work is the E(5) CPS [13]. Compared with the differential realization [13,30], the algebraic realization of the E(5) CPS was provided in [15,16] and is currently generalized to more general cases. Note that the algebraic version of the E(5) CPS is just the E(5) DS. To give a concrete application of the E(5) DS, we adopt the Hamiltonian [16]

$$\hat{H}_{\mathrm{E(5)}} = a\,\hat{C}_2[\mathrm{E(5)}] + b\,\hat{C}_2[\mathrm{SO(5)}] + c\,\hat{C}_2[\mathrm{SO(3)}] \tag{64}$$

with a, b, and c being adjustable parameters. To solve the E(5) Hamiltonian, one can expand the eigenstates as [16]

$$|\xi\,\tau\,\Delta L\rangle = \sum_{k=0}^{m} C_k^{\xi}(\hat{P}^{\dagger}_{l=2})^k|\tau\,\Delta L\rangle\,, \tag{65}$$

where C_k^{ξ} are the expansion coefficients with ξ denoting the additional quantum number used to distinguish different states with the same τ, Δ, and L values. Here, τ, Δ and L are the quantum numbers as same as those in the U(5) basis defined in (43). In principle, the dimension of the model space should be set to infinity due to the non-compactness of the E(5) group, which means that the number m could be taken as $m \to \infty$. Nevertheless, a nice scaling behavior of $\hat{C}_2[\mathrm{E(5)}]$ was revealed in [15]. The results suggest that a large enough value of m can guarantee the numerical solutions rather accurately. It would be convenient to rescale the parameter a in (64) with $a = \alpha m$ due to this scaling feature. More discussions on the solutions of the E(5) DS and their connections to the infinite square well potential adopted in the original E(5) CPS can be found in [15,16].

In experiments, ^{82}Kr can be taken as an example of the E(5) DS, as this nucleus was very recently suggested to be a candidate of the E(5) CPS for the U(5)-SO(6) shape phase transition [60]. In Figure 3, the low-lying level pattern of ^{82}Kr is shown to compare with the results solved from the Hamiltonian (64). For the $B(E2)$ transitions, the $E2$ transitional operator in theory is chosen as $\hat{T}^{\mathrm{E2}}_u = e(d^{\dagger} + \tilde{d})^{(2)}_u$ with the effective charge e

being determined by fitting the data for $B(E2;2_1^+ \to 0_1^+)$. Notably, the relative strength of $B(E2)$ transitions are only determined by the types of symmetry [2], which means that the $B(E2)$ ratios in the E(5) DS should be independent of the parameters a, b, c in the Hamiltonian. This point was confirmed in the concretely numerical calculations [15,16]. One can find from Figure 3 that the experimental data for ^{82}Kr are in good agreement with the results solved from the E(5) DS Hamiltonian (64) for both the level energies and the $B(E2)$ structure. Besides those in the $\xi = 1$ family, the states in the $\xi = 2$ family, 0_ξ^+ and 2_ξ^+, are also well reproduced by the theoretical calculations. A small deviation from the experiments may be the 3_1^+ state, to which the related $B(E2)$ transitions are accurately predicted but the excitation energy is overestimated in theory by about 0.5 MeV. It should be noted that the original E(5) CPS results including nearly the same $B(E2)$ structures as that shown in Figure 3 can be also applied to compare with the experimental data [60]. However, no energy degeneracy appearing in experiments indicates that the SO(5) symmetry is evidently broken in this nucleus. Removing the energy degeneracies in the E(5) mode can be naturally realized by the present Hamiltonian (64). The results confirm that the the low-lying dynamics in ^{82}Kr are indeed dominated by the E(5) DS [60].

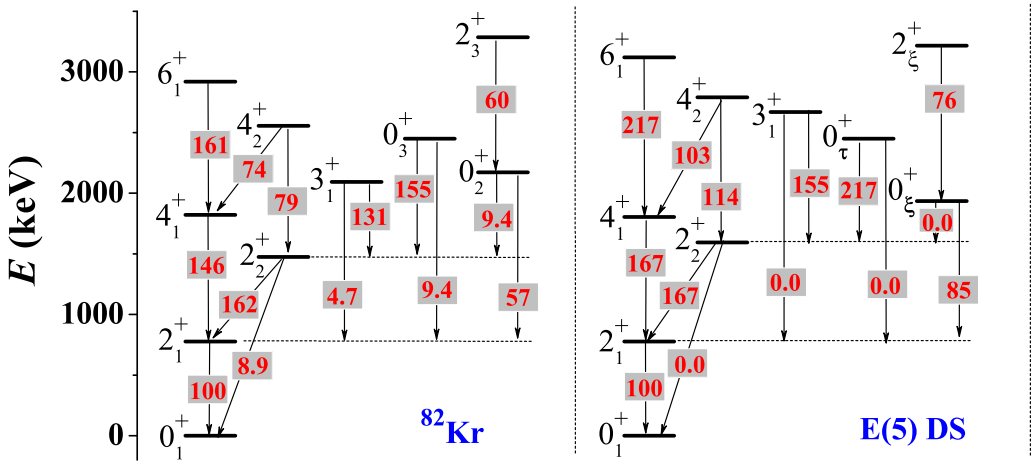

Figure 3. The low-lying structure of ^{82}Kr with the data taken from [60] is shown to compare with the results solved from the E(5) Hamiltonian in (64) with the truncation $m = 200$, $\alpha = 100.2$ keV, $b = 10$ keV and $c = 15$ keV. In the comparison, all the $B(E2)$ results have been normalized to $B(E2;2_1^+ \to 0_1^+) = 100$ (in any units), and 0_τ^+ and 0_ξ^+ (2_ξ^+) represent the ones in theory with $\xi = 1$ and $\xi = 2$, respectively.

6. Conclusions

In summary, a boson algebraic realization of the n-dimensional Euclidean group symmetry with $n = 2l + 1$ is proposed, by which the E(n) DS hidden in the 2^l-pole deformed system described by the U($n + 1$) vibron model is revealed. Along the group contraction, it is shown that the E(n) algebra may be equivalent to the SO($n + 1$) algebra in the large σ limit. More importantly, it has been justified that the E(n) DS can dynamically emerge at the critical point of the U(n)-SO($n + 1$) QPT under the condition that is strictly established in the classical limit and becomes a reasonable approximation for finite N. This point provides a solid theoretical basis for the CPS role of E(n) in describing this second-order QPT. This present study meanwhile generalizes our previous understanding of the E(5) DS for nuclear structure [15,16]. As a new test, an E(5) DS Hamiltonian is applied to reproduce the low-lying structure of ^{82}Kr. A good agreement between the experimental data and theoretical calculations confirms that the low-lying dynamics in this nucleus are indeed dominated by the E(5) DS, thus adding further empirical evidence of the Euclidean dynamical symmetry in experiments. It is worth mentioning that the E(3) DS [17] and E(2) DS [18] were also applied to explore nuclear properties. The former is just a specific case of E(n) with $n = 2l + 1$, but the latter with $n =$ even cannot be directly derived from

the present discussions. A boson realization of the E(2) algebras is given in [19] through considering a two-dimensional vector boson. The present analysis of $n =$ odd might be extended along this line to $n =$ even, which will be discussed elsewhere.

Author Contributions: Conceptualization, methodology, Y.Z.; software, Z.-T.W.; investigation, H.-D.J. and X.C. All authors have read and agreed to the published version of the manuscript.

Funding: This research was funded by the Natural Science Foundation of China under Grant No. 11875158, No. 12175097.

Institutional Review Board Statement: Not applicable.

Informed Consent Statement: Not applicable.

Data Availability Statement: Data are contained within the article.

Acknowledgments: We wish to thank Feng Pan for stimulating this work and for fruitful discussions on the related topics.

Conflicts of Interest: The authors declare no conflict of interest.

References

1. Iachello, F. *Lie Algebras and Applications*; Springer: Berlin/Heidelberg, Germany, 2006.
2. Iachello, F.; Arima, A. *The Interacting Boson Mode*; Cambridge University: Cambridge, UK, 1987.
3. Iachello, F.; Levine, R.D. *Algebraic Theory of Molecule*; Oxford University: Oxford, UK, 1995.
4. Leviatan, A. Partial dynamical symmetry in deformed nuclei. *Phys. Rev. Lett.* **1996**, *77*, 818–821. [CrossRef]
5. Leviatan, A. Partial dynamical symmetry at critical points of quantum phase transitions. *Phys. Rev. Lett.* **2007**, *98*, 242502. [CrossRef] [PubMed]
6. Garcìa-Ramos, J.E.; Leviatan, A.; Isacker, P.V. Partial dynamical symmetry in quantum Hamiltonians with higher-order terms. *Phys. Rev. Lett.* **2009**, *102*, 112502. [CrossRef]
7. Rowe, D.J. Quasidynamical symmetry in an interacting boson model phase transition. *Phys. Rev. Lett.* **2004**, *93*, 122502. [CrossRef]
8. Rowe, D.J.; Turner, P.S.; Rosensteel, G.A. Scaling properties and asymptotic spectra of finite models of phase transitions as they approach macroscopic limits. *Phys. Rev. Lett.* **2004**, *93*, 232502. [CrossRef] [PubMed]
9. Rowe, D.J. Phase transitions and quasidynamical symmetry in nuclear collective models: I. The U(5) to O(6) phase transition in the IBM. *Nucl. Phys. A* **2004**, *745*, 47–78. [CrossRef]
10. Bonatsos, D.; McCutchan, E.A.; Casten, R.F. SU(3) quasidynamical symmetry underlying the Alhassid-Whelan arc of regularity. *Phys. Rev. Lett.* **2010**, *104*, 022502. [CrossRef]
11. Bonatsos, D.; Karampagia, S.; Casten, R.F. Analytic derivation of an approximate SU(3) symmetry inside the symmetry triangle of the interacting boson approximation model. *Phys. Rev. C* **2011**, *83*, 054313. [CrossRef]
12. Alhassid, Y.; Whelan, N. Chaotic properties of the interacting-boson model: A discovery of a new regular region. *Phys. Rev. Lett.* **1991**, *67*, 816–819. [CrossRef]
13. Iachello, F. Dynamic symmetries at the critical point. *Phys. Rev. Lett.* **2000**, *85*, 3580–3583. [CrossRef]
14. Bohr, A.; Mottelson, B.R. *Nuclear Structure II*; Benjamin: Cambridge, NY, USA, 1975.
15. Zhang, Y.; Liu, Y.X.; Pan, F.; Sun, Y.; Draayer, J.P. Euclidean dynamical symmetry in nuclear shape phase transitions. *Phys. Lett. B* **2014**, *762*, 55–58. [CrossRef]
16. Zhang, Y.; Pan, F.; Liu, Y.X.; Luo, Y.A.; Draayer, J.P. Emergent dynamical symmetry at the triple point of nuclear deformations. *Phys. Rev. C* **2014**, *90*, 064318. [CrossRef]
17. Zhang, Y.; Hou, Z.F.; Chen, H.; Wei, H.Q.; Liu, Y.X. Quantum phase transition in the U(4) vibron model and the E(3) symmetry. *Phys. Rev. C* **2008**, *78*, 024314. [CrossRef]
18. Clark, R.M.; Macchiavelli, A.O.; Fortunato, L.; Krücken, R. Critical-point description of the transition from vibrational to rotational regimes in the pairing phase. *Phys. Rev. Lett.* **2006**, *96*, 032501. [CrossRef] [PubMed]
19. Zhang, Y.; Pan, F.; Liu, Y.X.; Draayer, J.P. The E(2) symmetry and quantum phase transition in the two-dimensional limit of the vibron model. *J. Phys. B* **2010**, *43*, 225101. [CrossRef]
20. Castaños, O.; Chacón, E.; Frank, A.; Moshinsky, M. Group theory of the interacting boson model of the nucleus. *J. Math. Phys.* **1979**, *20*, 35–44. [CrossRef]
21. Meyer-Ter-Vehn, J. The O(6) limit of the interacting boson model and its relation to triaxial nuclear models. *Phys. Lett. B* **1979**, *84*, 10–12. [CrossRef]
22. Kota, V.K.B. *SU(3) Symmetry in Atomic Nuclei*; Springer: Singapore, 2020.
23. Leschber, Y.; Draayer, J.P. Algebraic realization of rotational dynamics. *Phys. Lett. B* **1987**, *190*, 1–6. [CrossRef]
24. Castaños, O.; Draayer, J.P.; Leschber, Y. Shape variables and the shell model. *Z. Phys. A* **1988**, *329*, 33–43.
25. Draayer, J.P.; Weeks, K.J. Shell-model description of the low-energy structure of strongly deformed nuclei. *Phys. Rev. Lett.* **1983**, *51*, 1422–1425. [CrossRef]

26. Draayer, J.P.; Park, S.C.; Castaños, O. Shell-model interpretation of the collective-model potential-energy surface. *Phys. Rev. Lett.* **1989**, *62*, 20–23. [CrossRef] [PubMed]
27. Pan, F.; Draayer, J.P. New algebraic solutions for SO(6)-U(5) transitional nuclei in the interacting boson model. *Nucl. Phys. A* **1998**, *636*, 156–168. [CrossRef]
28. Pan, F.; Zhang, X.; Draayer, J.P. Algebraic solutions of an sl-boson system in the U(2l + 1)-O(2l + 2) transitional region. *J. Phys. A* **2002**, *35*, 7173–7185. [CrossRef]
29. Iachello, F.; Zamfir, N.V. Quantum phase transitions in mesoscopic systems. *Phys. Rev. Lett.* **2004**, *92*, 212501. [CrossRef] [PubMed]
30. Caprio, M.A.; Iachello, F. Analytic descriptions for transitional nuclei near the critical point. *Nucl. Phys. A* **2007**, *781*, 26–66. [CrossRef]
31. Alhassid, Y.; Whelan, N. Chaos in the low-lying collective states of even-even nuclei: Classical limit. *Phys. Rev. C* **1991**, *43*, 2637–2647. [CrossRef] [PubMed]
32. Cejnar, P.; Iachello, F. Phase structure of interacting boson models in arbitrary dimension. *J. Phys. A* **2007**, *40*, 581–595. [CrossRef]
33. Iachello, F. Analytic description of critical point nuclei in a spherical-axially deformed shape phase transition. *Phys. Rev. Lett.* **2001**, *87*, 052502. [CrossRef]
34. Casten, R.F.; Zamfir, N.V. Evidence for a possible E(5) symmetry in ^{134}Ba. *Phys. Rev. Lett.* **2000**, *85*, 3584–3586. [CrossRef]
35. Casten, R.F.; Zamfir, N.V. Empirical realization of a critical point description in atomic nuclei. *Phys. Rev. Lett.* **2001**, *87*, 052503. [CrossRef]
36. Clark, R.M.; Cromaz, M.; Deleplanque, M.A.; Descovich, M.; Diamond, R.M.; Fallon, P.; Firestone, R.B.; Lee, I.Y.; Macchiavelli, A.O.; Mahmud, H.; et al. Searching for X(5) behavior in nuclei. *Phys. Rev. C* **2003**, *68*, 037301. [CrossRef]
37. Clark, R.M.; Cromaz, M.; Deleplanque, M.A.; Descovich, M.; Diamond, R.M.; Fallon, P.; Lee, I.Y.; Macchiavelli, A.O.; Mahmud, H.; Rodriguez-Vieitez, E.; et al. Searching for E(5) behavior in nuclei. *Phys. Rev. C* **2004**, *69*, 064322. [CrossRef]
38. Iachello, F. Phase transitions in angle variables. *Phys. Rev. Lett.* **2003**, *91*, 132502. [CrossRef] [PubMed]
39. Bonatsos, D.; Lenis, D.; Petrellis, D.; Terziev, P.A. Z(5): critical point symmetry for the prolate to oblate nuclear shape phase transition. *Phys. Lett. B* **2004**, *588*, 172–179. [CrossRef]
40. Bonatsos, D.; Lenis, D.; Petrellis, D.; Terziev, P.A.; Yigitoglu, I. γ-rigid solution of the Bohr Hamiltonian for $\gamma = 30°4$ compared to the E(5) critical point symmetry. *Phys. Lett. B* **2005**, *621*, 102–108. [CrossRef]
41. Bonatsos, D.; Lenis, D.; Petrellis, D.; Terziev, P.A. X(3): an exactly separable γ-rigid version of the X(5) critical point symmetry. *Phys. Lett. B* **2006**, *632*, 238–242. [CrossRef]
42. Bonatsos, D.; Lenis, D.; Minkov, N.; Raychev, P.P.; Terziev, P.A. Sequence of potentials interpolating between the U(5) and E(5) symmetries. *Phys. Rev. C* **2004**, *69*, 044316. [CrossRef]
43. Caprio, M. Finite well solution for the E(5) Hamiltonian. *Phys. Rev. C* **2002**, *65*, 031304. [CrossRef]
44. Caprio, M. Consequences of wall stiffness for a β-soft potential. *Phys. Rev. C* **2004**, *69*, 044307. [CrossRef]
45. Fortunato, L. Soft triaxial rotovibrational motion in the vicinity of $\gamma = \pi/6$. *Phys. Rev. C* **2004**, *70*, 011302. [CrossRef]
46. Fortunato, L.; De Baerdemacker, S.; Heyde, K. Solution of the Bohr Hamiltonian for soft triaxial nuclei. *Phys. Rev. C* **2006**, *74*, 014310. [CrossRef]
47. Pietralla, N.; Gorbachenko, O.M. Evolution of the "β excitation" in axially symmetric transitional nuclei. *Phys. Rev. C* **2004**, *70*, 011304. [CrossRef]
48. Zhang, Y.; Pan, F.; Luo, Y.A.; Draayer, J.P. Critical point symmetry for the spherical to triaxially deformed shape phase transition. *Phys. Lett. B* **2015**, *751*, 423–429. [CrossRef]
49. Zhang, Y.; Pan, F.; Liu, Y.X.; Luo, Y.A.; Draayer, J.P. γ-rigid solution of the Bohr Hamiltonian for the critical point description of the spherical to γ-rigidly deformed shape phase transition. *Phys. Rev. C* **2017**, *96*, 034323. [CrossRef]
50. Budaca, R.; Budaca, A.I. Emergence of Euclidean dynamical symmetry as a consequence of shape phase mixing. *Phys. Lett. B* **2016**, *759*, 349–353. [CrossRef]
51. Budaca, R.; Buganu, P.; Budaca, A.I. Bohr model description of the critical point for the first order shape phase transition. *Phys. Lett. B* **2018**, *776*, 26–31. [CrossRef]
52. Iachello, F. Dynamic supersymmetries of differential equations with applications to nuclear spectroscopy. *Phys. Rev. Lett.* **2005**, *95*, 052503. [CrossRef]
53. Alonso, C.E.; Arias, J.M.; Vitturi, A. Critical-point symmetries in boson-fermion systems: the case of shape transitions in odd nuclei in a multiorbit model. *Phys. Rev. Lett.* **2007**, *98*, 052501. [CrossRef]
54. Zhang, Y.; Pan, F.; Liu, Y.X.; Hou, Z.F.; Draayer, J.P. Analytical description of odd-A nuclei near the critical point of the spherical to axially deformed shape transition. *Phys. Rev. C* **2010**, *82*, 034327. [CrossRef]
55. Zhang, Y.; Pan, F.; Liu, Y.X.; Luo, Y.A.; Draayer, J.P. Simple description of odd-A nuclei around the critical point of the spherical to axially deformed shape phase transition. *Phys. Rev. C* **2011**, *84*, 034306. [CrossRef]
56. Zhang, Y.; Pan, F.; Liu, Y.X.; Draayer, J.P. Critical point symmetries in deformed odd-A nuclei. *Phys. Rev. C* **2011**, *84*, 054319. [CrossRef]
57. Zhang, Y.; Pan, F.; Luo, Y.A.; Liu, Y.X.; Draayer, J.P. Critical-point symmetries in intermediately deformed odd-A nuclei. *Phys. Rev. C* **2012**, *86*, 044312. [CrossRef]
58. Chen, Y.X.; Jiang, H.; Dong, W.T.; Zhang, Y.; Pan, F.; Liu, Y.X.; Luo, Y.A. A triaxial critical point symmetry for odd-A nuclei. *Nucl. Phys. A* **2019**, *987*, 90–98. [CrossRef]

59. Zhang, Y.; Qi, B.; Zhang, S.Q. Critical point symmetry for odd-odd nuclei and collective multiple chiral doublet bands. *China Phys. Mech. Astron.* **2021**, *64*, 122011. [CrossRef]
60. Rajbanshi, S.; Bhattacharya, S.; Raut, R.; Palit, R.; Sajad, A.; Rajkumar, S.; Pai, H.; Babra, F.S.; Banik, R.; Bhattacharyya, S.; et al. Experimental evidence of exact E(5) symmetry in ^{82}Kr. *Phys. Rev. C* **2021**, *104*, L031302. [CrossRef]